ResearchOnline@JCU

JAMES COOK UNIVERSITY AUSTRALIA

This is the author-created version of the following work:

Chalak Qazani, Mohamad Reza, Asadi, Houshyar, and Nahavandi, Saeid (2021) ***A Motion Cueing Algorithm Based on Model Predictive Control Using Terminal Conditions in Urban Driving Scenario.*** **IEEE Systems Journal, 15 (1) pp. 445-453.**

Access to this file is available from:

https://researchonline.jcu.edu.au/86752/

© 2020 IEEE. Personal use of this material is permitted. Permission from IEEE must be obtained for all other uses, in any current or future media, including reprinting/republishing this material for advertising or promotional purposes, creating new collective works, for resale or redistribution to servers or lists, or reuse of any copyrighted component of this work in other works.

Please refer to the original source for the final version of this work:

https://doi.org/10.1109/JSYST.2020.2994154

A Motion Cueing Algorithm based on Model Predictive Control Using Terminal Conditions in Urban Driving Scenario

Mohammad Reza Chalak Qazani, Houshyar Asadi, *Member, IEEE*, Saeid Nahavandi, *Fellow, IEEE*

***Abstract*—The motion cueing algorithm (MCA) is in charge of the real vehicle motion feeling regeneration for the driver of the simulation-based motion platform (SBMP) with respect to its limitations. The model predictive control (MPC) has newly employed in developing MCAs to calculate the optimal input signals for delivering the best motion feeling to the SBMP's drivers while respecting the boundaries of the platform. The stability of the MCA based on MPC has become one of the main issues for some scenarios such as urban driving scenario which involves sudden decelerations/accelerations (stop and start moving), sharp and large turn, slalom movement. The urban driving scenario destabilises the current MCA based on MPC and leads undesired motion fluctuations which creates unpleasant motion artefact for the SBMP drivers. Therefore, the displacement of the SBMP should be penalised conservatively to respect the workspace boundaries for all driving scenarios. This will make the motion conservative and can cause some motion feeling error. In this paper, the concept of terminal conditions (weights and states) are employed for the first time to design and develop a new generation of MCA based on MPC to enhance the performance of the model for different scenarios such as the heavy-traffic scenario in urban areas. Also, the stability of the MPC by considering of the terminal conditions is investigated in MCA domain. Then, the MCA based on MPC by considering of terminal conditions is developed using MATLAB software with presentation of urban motion scenario. The outcomes demonstrate the effectiveness of the designed model with common MCA based on MPC without consideration of the terminal conditions.**

***Index Terms*— motion cueing algorithm, model predictive control, terminal conditions, simulation-based motion platform.**

I. Introduction

THE decrease of the cost, damages and time are the main reason for using the simulation-based motion platforms (SBMPs) in many areas such as industries and academic laboratories. The SBMPs can be used to study the driver behaviour, transportation, reliability of the autonomous vehicle, etc. [1, 2]. Unfortunately, the motion signal cannot be imported to the SBMP because of the boundaries of the SBMP [3-7]. Normally, the SBMPs have got a restricted workspace area compared with the real vehicles. The motion cueing algorithm (MCA) is in charge of the motion cues regeneration using the SBMP for producing the same motion feeling as a real vehicle while considering the SBMP's limitations.

The initial type of MCA was introduced by Conrad and Schmidt [8] known as classical MCA. The classical MCA composes of translational, rotational and tilt coordination channels. Cases et al. [9] used a genetic algorithm [10] to calculate the optimal indexes of the classical MCAs without practical evaluation. Also, Asadi et al. [11] used a particle swarm optimization algorithm to tun the classical MCA with better usage of workspace limitations. The second generation of the MCA is called adaptive MCA that varies the fixed parameters of the classical MCA [12]. Recently, different types of adaptive MCAs using the fuzzy logic control [13-15] are developed while considering the human vestibular system aiming to deliver the realistic motion feeling [16-18]. The linear quadratic regulator technique by considering of human vestibular to decrease the human feeling error is employed in forming of optimal MCA [19-21]. Asadi et al. [22] proposed a hybrid MCA with combination of classical and optimal MCAs to regenerate the compensation motion signal based the human motion sensation between real vehicle and SBMP user. Asadi et al. [2] employed the genetic algorithm along with the linear quadratic regulator to extract the robust optimal MCA while considering the system nonlinearities. The idea of the optimal MCA by considering of the SBMP limitations is also introduced by Dagdelen et al. [23] known as MCA based on model predictive control (MPC). As the provided model [23] was not able to tilt the driver's head based on human vestibular model, the SBMP could easily hit the boundaries. An explicit MPC was employed to generate the MCA for a SBMP with 2 degree of freedom (2-DoF) by Fang and Kemeny [24]. They employed the multi-parametric toolbox of MATLAB to find the affine function. The practical comparison of the MCA based on MPC and classical MCA is investigated by Krupchanka et al. [25] which proves the preferable performance of the MCA based on MPC. In order to improve the performance of the mechanism as well as lowering the computational burden, Mohammadi et al. [26] employed the genetic algorithm to extracted the best prediction and control horizons of the MPC. Rengifo et al. [27] used the recurrent neural network approach to reduce the computational burden of the MCA based on MPC using a proper learning rate tuning. Qazani et al. [28] established the new MCA based on MPC with capability of decoupling the tilt

(*Corresponding author: Mohammad Reza Chalak Qazani*)
The authors are with the Institute for Intelligent Systems Research and Innovation, Deakin University, Geelong, VIC 3216, Australia (e-mail: m.r.chalakqazani@gmial.com; Houshyar.asadi@deakin.edu.au; saeid.nahavandi@deakin.edu.au).

angle from angular displacement (AD) to produce the more accurate motion signal for mid-sized SBMPs. Qazani et al. [29, 30] introduced two novel mechanism to work as an SBMP with high fidelity, but they are not still suitable for urban driving scenarios including accelerations and deaccelerations and large turns because of skipping the consideration of the terminal conditions. Recently, Qazani et al. [31, 32] established the time-varying MCA based on MPC with ability of considering the nonlinearities of the mechanism. The real-time application of the time-varying MPC is hard to be implemented due to the high computational load for updating the MPC states based on the present configuration of the end-effector.

All the above-mentioned research studies on MCAs based on MPC [23-28] only considered when the vehicle is driving on the roads without any traffic jam or traffic lights, and without applying much starting and stopping signals. Using the urban driving scenarios which involve traffic lights, interaction with other drivers and pedestrians, roundabouts and puddles of the road can destabilise the previous models [23-28] and cause undesired platform fluctuations due to the absence of terminal conditions (weights and states). Therefore, they [23-28] should be penalised conservatively to respect the workspace area of the SBMPs, but this hypothesis reduces the better usage of the workspace area and enhances the motion feeling error for the driver of the SBMP. Also, the stability of their models [23-28] cannot be guaranteed as the end-effector cannot turn back to the natural position at the end of the prediction horizon without using the terminal states. Terminal conditions only implemented in the time-varying MCA based on MPC by Qazani et al. [31, 32], however the time-varying MPC cannot regenerated the real-time motion cues in heavy traffic jam as it has a high computational burden to extract the optimal input signal.

In this study, the Hexapod SBMP, which is shown in Fig. 1, is employed to produce the regenerated motion signal via MCA. Inverse kinematics problem is used to extract the pod length $(\boldsymbol{l_i})$ of the Hexapod SBMP based on the desired configurations of the SBMP [33]. The PID controller is used to find the required control actions of the actuators $(\boldsymbol{F_i})$ based on the calculated actuator positions via inverse kinematics unit and the feedbacks of pod positions $(\boldsymbol{l_i^{FB}})$ and velocities $(\boldsymbol{\dot{l}_i^{FB}})$.Also, a new linear MCA based on MPC with considering terminal conditions shown as WTR is designed to produce realistic results when there is a heavy-traffic motion scenario. The main advantage of the investigated model is the power of controlling the terminal conditions to stabilise the model when there is a heavy-traffic motion scenario in comparison with the MCA based on MPC without considering terminal conditions shown as WOTR. In addition, developing a new MCA based on MPC using terminal states causes the end-effector to return to the natural position at the end of the prediction horizon, and terminal weighting parameters to increase to respect the SBMP workspace boundaries. Eventually, the proposed MCA based on MPC checks the terminal conditions of the system to respect the SBMP workspace boundaries. The stability of the MPC can be investigated via *Terminal States* [34, 35], *Infinite Output Prediction Horizon* [36] and *Terminal Weighting Matrix* [37, 38]. The stability of the investigated model is studied through

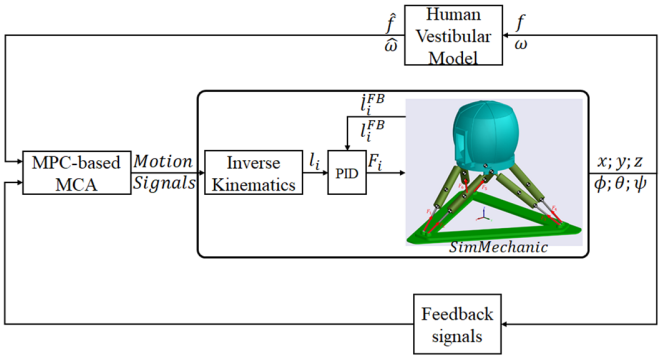


Fig. 1. The schematic model of the MCA based on MPC in Simulink/MATLAB software using Hexapod SBMP

terminal conditions using the convergence of the motion feeling error.

The human vestibular model, which is responsible for the understanding of the motion feeling is described in section II. The MCAs based on MPC WTR and WOTR are explained in section III. In section IV, the investigated model is designed and developed, and the outcomes show the effectiveness of the investigated model in comparison with existing MCAs based on MPC. In section V, the foundations of the research are remarked.

II. The Human Vestibular System

The human vestibular model is a member of the motion perceptual system of the human body that is responsible for the postural stability and integrating balance of the body as well as detecting the motion signals. The human vestibular system composes of the semicircular systems and otolith organs which are situated inside the inner ear of the human body [39, 40]. The human vestibular system perceives the rotational and translational motion signals using the semicircular systems and otolith organs, respectively.

The otolith organs perceive the linear acceleration (LA) signal known as sensed specific force (SSF) as follows:

$$\mathbf{S}_F = \begin{cases} a_x - g\sin\theta \\ a_y - g\sin\phi\cos\theta \\ a_z - g\cos\phi\cos\theta \end{cases} \quad (1)$$

where $\mathbf{a}$ is the LA signal and g is the gravity acceleration. Also, ϕ, θ and ψ are *roll*-, *pitch*- and *yaw*-angle.

The best mathematical models of the human semicircular systems and otolith organs models based on the studies of Asadi et al. [39, 40] are:

$$\frac{\hat{\omega}}{\omega} = \left(\frac{\tau_1\tau_a s^2}{(1+\tau_a s)(1+\tau_1 s)}\right) \quad (2)$$

$$\frac{\hat{\mathrm{f}}(s)}{\mathrm{f}(s)} = K_{OTO}\left(\frac{(\tau_L s+1)}{(\tau_2 s+1)(\tau_3 s+1)}\right) \quad (3)$$

where $\hat{\omega}$ is the sensed angular velocity (SAV), $\hat{\mathrm{f}}$ is SSF, τ_1 = 6.1, 5.3, 10.2 (s) along *roll*-, *pitch*- and *yaw*-angle, τ_a=30 (s) in all three angular directions, τ_L = 5.3, 5.33, 5.33 (s) in the *x*-, *y*- and *z*-axis, K_{OTO}=0.4, τ_2=0.016 (s) and τ_3=13.2 (s) in all three translational directions.

The human vestibular state space model can be formulated by combining Eq. (2) and Eq. (3) in the state space form as:

$$\dot{\mathbf{x}}_V = \mathbf{A}_V\mathbf{x}_V + \mathbf{B}_V\mathbf{u} \quad (4.a)$$

$$\hat{\mathbf{y}}_{\mathrm{V}} = \mathbf{C}_{\mathrm{V}}\mathbf{x}_{\mathrm{V}} + \mathbf{D}_{\mathrm{V}}\mathbf{u} \quad (4.b)$$

where $\mathbf{u}$, $\hat{\mathbf{y}}_{\mathrm{V}}$ and $\mathbf{x}_{\mathrm{V}}$ are the input vector including angular velocity (AV) and LA signals which are the best inputs based on the conducted work by Houck et al. [41], output vector including SAV and SSF, and state vector of the human vestibular model, respectively. The presented human vestibular model in Eq. (4) is used in developing the proposed MCA based on MPC in the following section.

III. MCAs BASED ON MPC WTR AND WOTR

A. Verification of the Model

As the human vestibular model in Eq. (4) is continues, it should be discretised based on time step (0.01 second) to be applied for the MPC model as bellow:

$$\mathbf{x}_{\mathrm{V}}(t+1) = \mathbf{A}_{\mathrm{V}}\mathbf{x}_{\mathrm{V}}(t) + \mathbf{B}_{\mathrm{V}}\mathbf{u}(t) \quad (5.a)$$

$$\hat{\mathbf{y}}_{\mathrm{V}}(t) = \mathbf{C}_{\mathrm{V}}\mathbf{x}_{\mathrm{V}}(t) \quad (5.b)$$

It should be noted that only semicircular model has $\mathbf{D}_{\mathrm{V}}$ matrix. Then, $\mathbf{D}_{\mathrm{V}}$ can be eliminated from Eq. (5) with implementing one time-step delay to the semicircular model after discretisation. In order to control the linear displacement (LD), linear velocity (LV) and AD of the SBMP, these parameters should be calculated based on the input signal which are AV and LA signals. The below relation is employed to extract the LD, LV and AD of the SBMP.

$$\mathbf{x}_{\mathrm{d}}(t+1) = \mathbf{A}_{\mathrm{d}}\mathbf{x}_{\mathrm{d}}(t) + \mathbf{B}_{\mathrm{d}}\mathbf{u}(t) \quad (6)$$

where $\mathbf{x}_{\mathrm{d}}$ is the state vector of the integration state space model which includes $[x \quad V_x \quad \theta \quad y \quad V_y \quad \phi \quad z \quad V_z \quad \psi]^{\mathrm{T}}$, $\mathbf{A}_{\mathrm{d}}$ and $\mathbf{B}_{\mathrm{d}}$ are the matrices of the integration state space model which can be found in [31]. Also, x, y and z are argument of LD vector; V_x, V_y and V_z are argument of LV vector; and ϕ, θ and ψ are argument of AD vector.

The discretised MPC state space model can be extracted by combining discretised model in Eq. (5) and Eq. (6) to be employed in both models including WTR and WOTR as:

$$\mathbf{x}_{\mathrm{m}}(t+1) = \mathbf{A}_{\mathrm{m}}\mathbf{x}_{\mathrm{m}}(t) + \mathbf{B}_{\mathrm{m}}\mathbf{u}(t) \quad (7.a)$$

$$\mathbf{y}(t) = \mathbf{C}_{\mathrm{m}}\mathbf{x}_{\mathrm{m}}(t) \quad (7.b)$$

where $\mathbf{x}_{\mathrm{m}} = [\mathbf{x}_{\mathrm{V}} \quad \mathbf{x}_{\mathrm{d}}]^{\mathrm{T}}$ is state vector, and $\mathbf{y}$ is output vector of the MPC model including motion sensation, LD, LV and AD. Also, $\mathbf{A}_{\mathrm{m}}$, $\mathbf{B}_{\mathrm{m}}$ and $\mathbf{C}_{\mathrm{m}}$ are the final matrices of the discretised MCA state space model. The augment state space model of the Eq. (7) can be defined as:

$$\mathbf{x}(t+1) = \mathbf{A}\mathbf{x}(t) - \mathbf{B}\Delta\mathbf{u}(t) \quad (8.a)$$

$$\mathbf{y}(t) = \mathbf{C}\mathbf{x}(t) \quad (8.b)$$

where control input $\Delta\mathbf{u}(t)$ is $\mathbf{u}(t) - \mathbf{u}(t-1)$, the state $\mathbf{x}(t)$ is $[\mathbf{x}_{\mathrm{m}}(t) - \mathbf{x}_{\mathrm{m}}(t-1) \quad \mathbf{y}(t)]^{\mathrm{T}}$ and matrices $\mathbf{A}$, $\mathbf{B}$ and $\mathbf{C}$ are:

$$\mathbf{A} = \begin{bmatrix} \mathbf{A}_{\mathrm{m}} & \mathbf{0} \\ \mathbf{C}_{\mathrm{m}}\mathbf{A}_{\mathrm{m}} & \mathbf{I} \end{bmatrix}, \mathbf{B} = \begin{bmatrix} \mathbf{B}_{\mathrm{m}} \\ \mathbf{C}_{\mathrm{m}}\mathbf{B}_{\mathrm{m}} \end{bmatrix}, \mathbf{C} = [\mathbf{0} \quad \mathbf{I}] \quad (9)$$

The cost function, $\mathbf{J}(t)$, is formulated to decrease the motion sensation error of the SBMP driver in comparison with real vehicle driver. Also, the reference signal, $\mathbf{R}_{\mathrm{s}}$, should be specified in order to define the cost function. There are two approaches for definition of the reference signal known as time-invariant and time varying. In this study, the time-invariant reference signal along with the prediction horizon is considered. The reason is time-varying reference signal enhances the chance of instability if there is a discrepancy between the actual motion signal and the predicted motion signal. If the state at the n time-step (T_s) is indicated by $\mathbf{x}(t+n|t)$, the cost function by considering of the terminal condition can be calculated as:

$$\mathbf{J}(t) = \sum_{i=1}^{N_p-1}\left(\mathbf{R}_{\mathrm{s}}(t+i|t) - \mathbf{y}(t+i|t)\right)^{\mathrm{T}}\mathbf{Q}\left(\mathbf{R}_{\mathrm{s}}(t+i|t) - \mathbf{y}(t+i|t)\right) + \sum_{i=1}^{N_c-1}\mathbf{u}^{\mathrm{T}}(t+i|t)\mathbf{S}\mathbf{u}(t+i|t) + \sum_{i=1}^{N_c-1}\Delta\mathbf{u}^{\mathrm{T}}(t+i|t)\mathbf{R}\Delta\mathbf{u}(t+i|t) + \left(\mathbf{R}_{\mathrm{s}}\left(t+N_p|t\right) - \mathbf{y}\left(t+N_p|t\right)\right)^{\mathrm{T}}\mathbf{Q}_{N_p}\left(\mathbf{R}_{\mathrm{s}}\left(t+N_p|t\right) - \mathbf{y}\left(t+N_p|t\right)\right) \quad (10)$$

where N_p and N_c are the prediction horizon and control horizon, respectively. Also, $\mathbf{R}$, $\mathbf{S}$, and $\mathbf{Q}$ are the diagonal weighting matrices for the input rate, input and output, respectively. It should be noted that $\mathbf{Q}_{N_p}$ is terminal weighting matrices for the outputs using terminal conditions, and based on the Riccati equation it can be calculated as:

$$\mathbf{Q}_{N_p} = \mathbf{A}^{\mathrm{T}}\mathbf{Q}_{N_p}\mathbf{A} - \mathbf{A}\mathbf{Q}_{N_p}\mathbf{B}\left(\mathbf{B}^{\mathrm{T}}\mathbf{Q}_{N_p}\mathbf{B} + \mathbf{R}\right)^{-1}\mathbf{B}^{\mathrm{T}}\mathbf{Q}_{N_p}\mathbf{A} + \mathbf{Q}. \quad (11)$$

The Eq. (11) should be used to find the terminal weighting matrices using terminal conditions. Then, if the existing MCA based on MPC WOTR is employed [23-28], the terminal weighting matrices is the same as the previous weighting matrices which is $\mathbf{Q}$ in Eq. (10).

Another difference between the existing MCA based on MPC WOTR and proposed MCA based on MPC WTR is the constraints of the state in the terminal points which should be equal to zero as follows:

$$\mathbf{x}\left(t+N_p\mathrm{T}_{\mathrm{s}}\right) = \mathbf{0} \quad (12)$$

In other words, Eq. (12) helps the SBMP to move back to the neutral position once it reaches to the end of the prediction horizons. It enhances the efficiency of the investigated model because as the SBMP workspace boundaries will be respected more without using any conservative weighting parameters.

Finally, the limitation of the inputs' rates, inputs and outputs should be categorised into three different sets to be respected on the optimisation process as:

$$\begin{bmatrix} \mathbf{M_1} \\ \mathbf{M_2} \\ \mathbf{M_3} \end{bmatrix}\Delta\mathbf{U} \leq \begin{bmatrix} \mathbf{n_1} \\ \mathbf{n_2} \\ \mathbf{n_3} \end{bmatrix} \quad (13)$$

where $\mathbf{M_1}$ and $\mathbf{n_1}$ are the constraints on inputs' rates, $\mathbf{M_2}$ and $\mathbf{n_2}$ are the constraints on inputs, and $\mathbf{M_3}$ and $\mathbf{n_3}$ are the constraints on outputs.

B. Stability Analysis

One of the common techniques to stabilise the MPC model is called *Terminal State* which means that the states of the system limit to zero at the end of the prediction horizon. It will be achieved by defining extra constraints [34, 35]. The same methodology is followed in this paper to prove the stability of the proposed MCA based on MPC. Also, selecting the long prediction horizons can stabilise the MPC WOTR same to *Infinite Output Prediction Horizon* [36]. The third method to stabilise the MPC model is the definition of the *Terminal Weighting Matrix* [37, 38], which is followed in this study simultaneously with the definition of the terminal states. Also, there are some other ways to prove the stability of the MPC WOTR with decaying the absolute value of system states [42].

The feedback control law $\mathbf{u}(t)$ can be determined as:

$$\mathbf{u}(t) = -\mathbf{R}^{-1}\mathbf{B}^{\mathrm{T}}\mathbf{P}^{-1}\left(t+\mathrm{T_s}, t+N_p\mathrm{T_s}\right)\mathbf{A}\mathbf{x}(t) \quad (14)$$

where $\mathbf{P}^{-1}$ can be calculated using the Riccati equation as:

$$\mathbf{P}(t+k|t) = \mathbf{A}^{-1}\mathbf{P}(t+k+1|t)\mathbf{A}^{-1^{\mathrm{T}}} - \mathbf{A}^{-1}\mathbf{P}(t+k+1|t)\mathbf{A}^{-1^{\mathrm{T}}}\mathbf{C}^{\mathrm{T}}\mathbf{E}^{\mathrm{T}}\left[\mathbf{I} + \mathbf{E}\mathbf{C}\mathbf{A}^{-1}\mathbf{P}(t+k+1|t)\mathbf{A}^{-1^{\mathrm{T}}}\mathbf{C}^{\mathrm{T}}\mathbf{E}^{\mathrm{T}}\right]^{-1}\mathbf{E}\mathbf{C}\mathbf{A}^{-1}\mathbf{P}(t+k+1|t)\mathbf{A}^{-1^{\mathrm{T}}} + \mathbf{B}\mathbf{R}^{-1}\mathbf{B}^{\mathrm{T}} \quad (15)$$

where $\mathbf{P}$ can be calculated using Eq. (15) with reverse summation from N_p to 1 time-step. Also, $\mathbf{P}(t+\mathrm{T_s}, t+\mathrm{T_s})$ is equal to zero as an extra constraint of the system.

It should be noted that the prediction horizon N_p is defined sufficiently long to find the feedback control law in Eq. (14). The control law extracted from Eq. (14) (as a feedback control law of the system) is stable, if the system in Eq. (8) is controllable and observable. Then, under controllability of the $\mathbf{A}$ and $\mathbf{B}$, and observability of $\mathbf{A}$ and $\mathbf{C}$, the stability of the system in Eq. (8) using terminal states can be proven using *Theorem 1* and *Theorem 2* of Kwon and Pearson [35].

Both MCAs based on MPC WTR and WOTR are tuned based on following procedure to have the wise consummation of the workspace.

- First, the MPC horizons should be tuned to reduce the computational burden of the system and reach better results.
- At the second step, the inputs' rates, inputs and outputs weights are tuned to decrease the motion feeling error between the real and simulated vehicle and respect the limitations of the SBMP.
- Lastly, the scale factors (SFs) are defined to ensure the workspace boundaries of the SBMP will not be exceeded.

The workspace boundaries of the Hexapod SBMP using in this study are provided in Table I. Table II shows the tuning parameters including SFs, MPC horizons and weighting indexes of the MCAs based on MPC WTR and WOTR, respectively.

IV. Results and Discussions

Both investigated MPC models including WTR and WOTR are designed in MATLAB software and the schematic representation of the proposed algorithm is shown in Fig. 1. Therefore, user or driver of the SBMP and user or driver of the real car, are both simulated in the Simulink environment. The model includes MCA, inverse kinematics problem [6], PID controller unit and SimMechanic model. The MCA block is designed based on the developed model in section III. The developed MPC model is very fast because it is designed using MPC toolbox of the MATLAB software using KWIK algorithm [43] to find the optimal input signal. Also, the SimMechanic representation of the Hexapod is developed using the geometrical and dynamical indexes of the mechanism [44]. It enhances the ability of the model to reproduce the motion signals as close as possible to the real Hexapod SBMP.

TABLE I
THE WORKSPACE BOUNDARIES OF THE HEXAPOD SBMP

Index	Position		Velocity		Acceleration	
	Amp	unit	Amp	unit	Amp	unit
x	±0.07	m	±1.3	m/s	±25	m/s^2
y	±0.05	m	±1.3	m/s	±25	m/s^2
z	±0.03	m	±0.9	m/s	±40	m/s^2
Roll	±7.95	rad	±35.6	rad/s	±191	rad/s^2
Pitch	±7.95	rad	±19.4	rad/s	±191	rad/s^2
Yaw	±6.36	rad	±19.4	rad/s	±76.4	rad/s^2

Amp: amplitude; m: meter; rad: radium; s: second;

The heavy-traffic motion scenario in the urban area is recorded using Rigs of Rods version 0.39.5 (vehicle simulation environment) for 500 seconds. Fig. 2.a-b presents the LA and AV input driving motion signal after multiplying to SF from 300 to 400 seconds of the motion scenario along three directions, respectively. The same SFs should be employed to reach the fair comparison between two methods using WTR and WOTR which are shown in Table II [45, 46].

The outcomes of the MCA based on MPC WTR for motion signals for 500 seconds has been evaluated using root mean square error (RMSE) and correlation coefficient (CC). The RMSE of the motion feeling between the SBMP and the real car's drivers is presented in Table III. It is shown that the RMSE of the SSF using MCA based on MPC WTR improves 19.8, 38.9 and 20.7 percent along *x*-, *y*- and *z*-axis compared with MCA based on MPC WOTR. It is due the fundamental improvement of the terminal conditions' consideration inside

TABLE II
THE TUNING INDEXES OF THE MCAS BASED ON MPC WOTR AND WTR.

Index	Longitudinal channel		Lateral channel		Yaw channel		Heave channel	
	WOTR	WTR	WOTR	WTR	WOTR	WTR	WTR	WTR
N_p	150	150	150	150	150	150	150	150
N_c	3	3	3	3	3	3	3	3
Linear SF	1/5	1/5	1/5	1/5	NA	NA	1/3	1/3
Angular SF	1	1	1	1	1/2	1/2	NA	NA
SSF	1000	1000	850	850	NA	NA	65	65
LD	1.4×10^4	1.4×10^3	1.24×10^4	1.4×10^3	NA	NA	850	150
LV	10	5	10	5	NA	NA	10	5
LA	10^{-4}	10^{-4}	10^{-4}	10^{-4}	NA	NA	10^{-4}	10^{-4}
Linear Jerk	1	1	1	1	NA	NA	1	1
SAV	6.5×10^3	6.5×10^3	5×10^3	5×10^3	1.95×10^3	1.95×10^3	NA	NA
AD	200	75	200	75	725	725	NA	NA
AV	0.1	0.1	0.1	0.1	0.1	0.1	NA	NA
Angular Acceleration	1	1	1	1	1	1	NA	NA

TABLE III
THE OUTCOMES FOR THE MCAS BASED ON MPC WTR AND WOTR.

Index	RMSE		CC	
	WOTR	WTR	WOTR	WTR
OTO a_x	0.4489	0.3600	0.6401	0.7847
OTO a_y	0.2984	0.1821	0.8199	0.9368
OTO a_z	0.2098	0.1663	0.4301	0.5047
SCC *roll-dot*	0.0605	0.0476	0.5022	0.8186
SCC *pitch-dot*	0.0759	0.0810	0.2996	0.6063
SCC *yaw-dot*	0.0610	0.0645	0.9034	0.8954

OTO: Otolith Organ; SCC: Semicircular System.

the QP problem. Using terminal consideration guarantees returning of the end-effector to the neutral position at the end of the prediction horizon [47]. The MCA based on MPC WOTR is not suitable for regeneration of the motion signals because it should be penalised more than MCA based on MPC WTR to respect the workspace boundaries. Also, CC shows the shape following the sameness of the motion feeling between the drivers of the SBMP and the real car. Asadi et al. [2, 17] employed CC in MCA domain as an essential factor to evaluate the motion feeling of MCA. The range of the CC is between -1 and 1 while one shows the identical shape sameness between two signals.

The motion feelings of the AV and LA signals along *x*-, *y*- and *z*-axis for the actual vehicle driver and SBMP driver using both MCAs based on MPC WTR and WOTR are shown in Fig. 3.a-f from 350 to 380 seconds of the motion. The period of recorded driving including most aggressive generated driving signal such as acceleration, deacceleration, sharp turning and puddles of the road is selected for testing and validation of the proposed algorithm. The better follow of the motion feeling signal for the AV along *pitch*-, *roll*- and *yaw*-angle using MCA based on MPC WTR is shown in Fig. 3.a-b. Also, Fig. 3.d-f show the SSF along *x*-, *y*- and *z*-axis. Fig. 3.d-f shows the better shape sameness of the SSF using MCA based on MPC WTR compared with MCA based on MPC WOTR which improves 22.6, 14.2 and 17.3 per cent along *x*-, *y*- and *z*-axis, respectively. The MCA based on MPC WOTR has a high weighting parameter along *x*-, *y*- and *z*-axis because of the employment of the heavy-traffic motion scenario to keep the end-effector inside the workspace area. The MCA based on MPC WTR respects the workspace boundaries and it returns the SBMP to the neutral position at the end of prediction horizon [47]. This capability has enhanced the ability of the proposed method to regenerate the more accurate motion signals without producing any motion artefacts.

Fig. 4.a-f demonstrates the error of the motion feeling for AV and LA signals along *x*-, *y*- and *z*-axis for the driver in the real world and the driver of the SBMP using both MCAs based on MPC WTR and WOTR from the 350 to 380 seconds. Fig. 4.a shows that the SAV along *pitch*-angle increases 6 per cent using the proposed method. It is due to the improvement of the SSF along *x*-axis which needs the more regeneration of the sustainable low-frequency motion signal. Fig. 4.b shows that the motion feeling error of the AV signals reduces using MCA based on MPC WTR more than 21 per cent along *roll*-angle. The error of the SAV along yaw-angle remains the same based on Fig. 5.c. Also, the error of the SSF along *x*-, *y*- and *z*-axis are

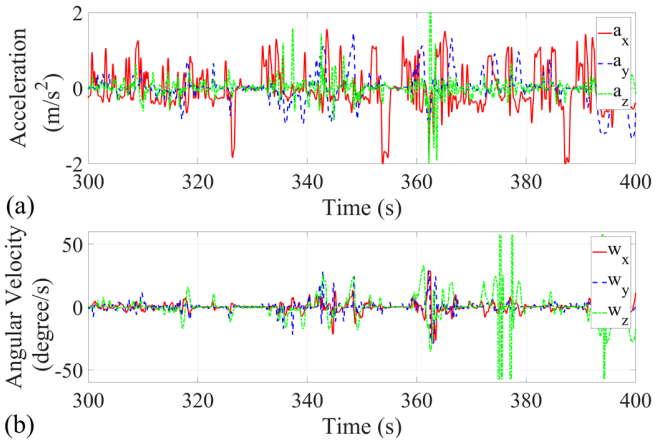


Fig. 2. The heavy-traffic urban motion scenario along three directions: (a) LA; (b) AV.

reduced using the proposed MCA based on MPC WTR based on Fig. 4.d-f, respectively, as presented in the second column of Table III.

Fig. 5.a-c shows the LD of the SBMP WTR and WOTR. According to the figures, the end-effector can move wisely inside the workspace area and respect the limitations using MCA based on MPC WTR. However, the MCA based on MPC WOTR should be penalised to respect the workspace boundaries, which can make the motion conservative and consequently cause feeling error. The better usage of the workspace area using MCA based on MPC WTR is the main reason for the improvement of the proposed method. Also, Fig. 5.d-f shows the AD of the end-effector using both proposed methods. The proposed method can use the AD of the end-effector slightly more and can generate the low-frequency sustainable motion signal better than the previous method. It should be noted that the better usage of the AD of the end-effector is due to the definition of the terminal weighting parameters instead of selecting conservative weights.

The large pulse signal which is 10 m/s^2 is also applied to both MCAs based on MPC WTR and WOTR to practically show the stability and returning capability of the platform to neutral position using proposed and existing methods. Fig. 6.a-b shows the SAV and SSF of the actual driver and driver of the SBMP using the proposed and existing MCAs based on MPC. The motion feeling resulted from a big acceleration/deacceleration motion signal using the MCA based on MPC WTR enhances the RMSE of motion feeling error for LA signal along x-axis and AV signal along pitch angle 76.13 and 11.82 per cent, respectively, compared with the MCA based on MPC WOTR. The neglection of the terminal weighting parameters and the terminal states are the main reason that the SSF and SAV using MCA based on MPC WOTR undesirably fluctuate and increase the motion feeling error as shown in Fig. 6.c-d. Fig. 6.e-f show the lengths of pods using both MCAs based on MPC WOTR and WTR, respectively. The MCA based on MPC WOTR reaches the pod length limitation at 5.7 (s) of the pulse motion scenario. However, even saturation of the pod length does not help the algorithm to keep the end-effector inside the workspace boundaries, and the passive joints hit their limitations at 5.7 (s)

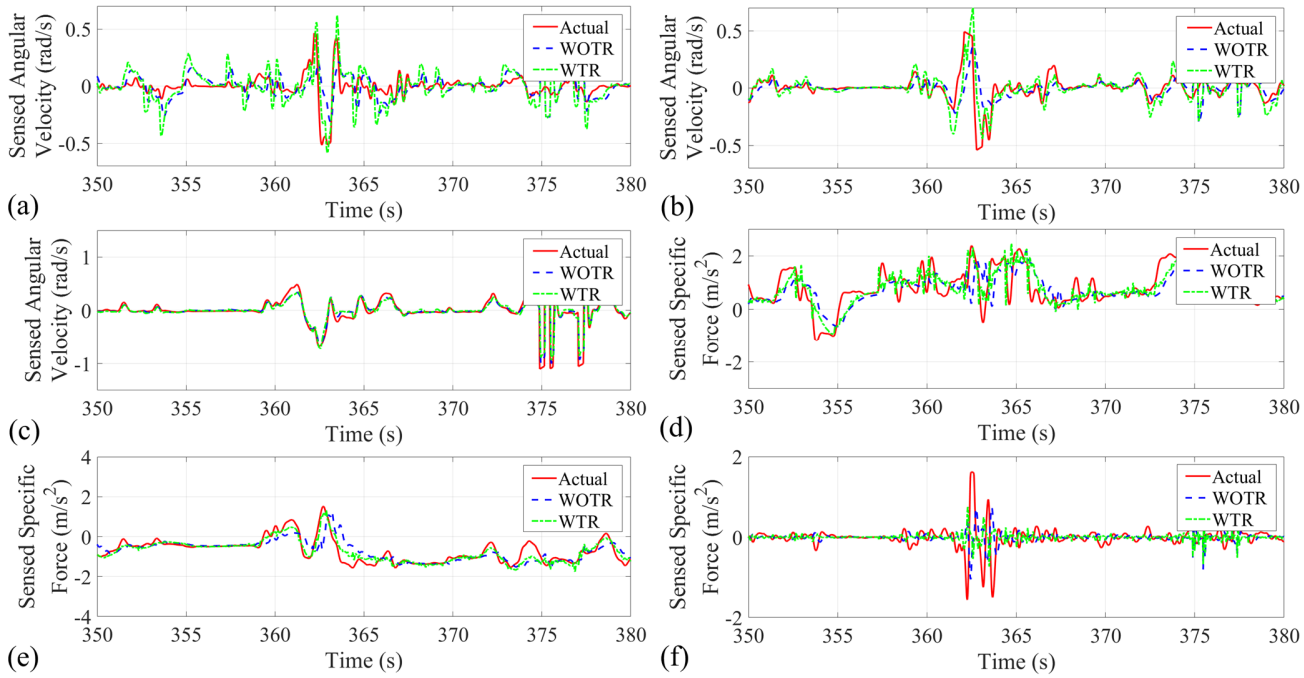


Fig. 3. The SAV and SSF for the both MCAs based on MPC WTR and WOTR during the 350-380 seconds of the motion scenario along: (a) *pitch*-angle; (b) *roll*-angle; (c) *yaw*-angle; (d) *x*-axis; (e) *y*-axis; (e) *z*-axis.

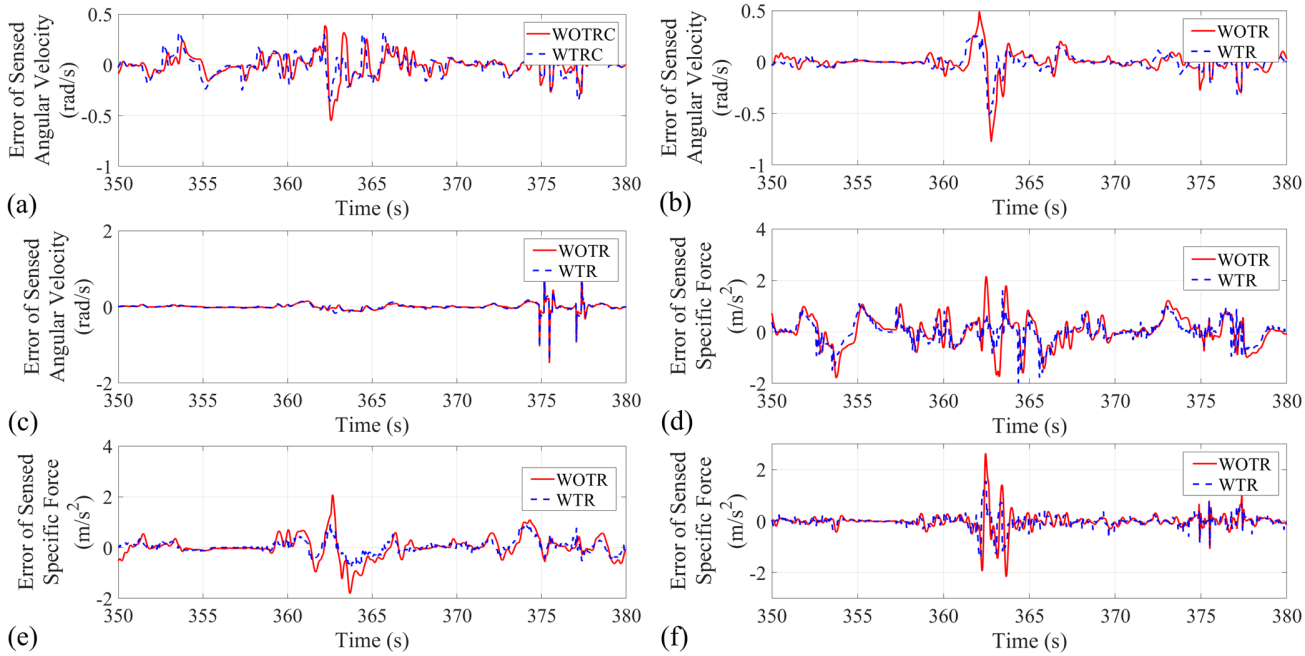


Fig. 4. The SAV and SSF errors between the real and SBMP drivers for the both MCAs based on MPC WTR and WOTR during the 350-380 seconds of the motion scenario along: (a) *pitch*-angle; (b) *roll*-angle; (c) *yaw*-angle; (d) *x*-axis; (e) *y*-axis; (e) *z*-axis.

of the motion scenario. The motion signal can be followed via MCA based on MPC WOTR. The regeneration of the motion signal using MCA based on MPC WOTR shows the consequences of neglecting the terminal conditions. Using the existing method, the end-effector finally configurates to the wrong position because of violating the limitations of the passive joints and caused false motion cues as shown in Fig. 6.c does not turn back to zero after the deacceleration. The Fig. 7 shows the final configuration of the Hexapod SBMP using MCA based on MPC WOTR. Fig. 7 shows that the configuration of the end-effector is lost, and the end-effector cannot turn back to the neutral position which is one of the main problems of the existing methods.

The newly proposed MCA based on MPC results in the better

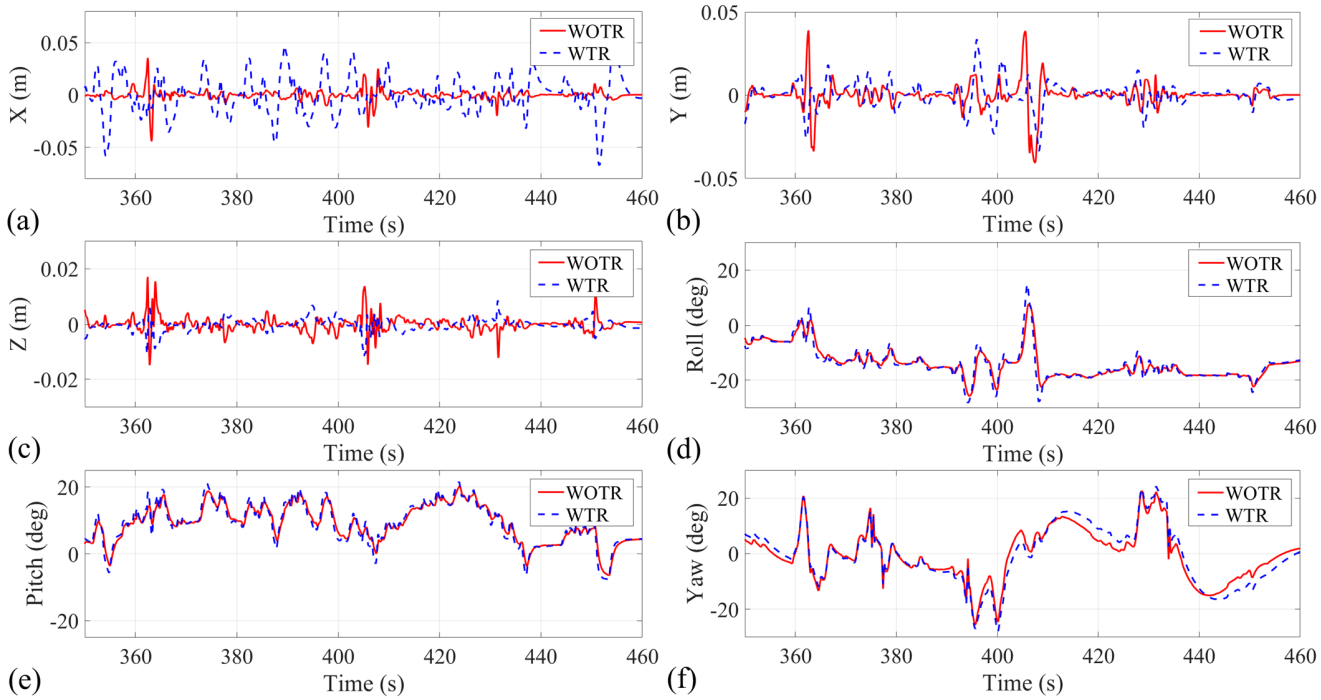


Fig. 5. The LD and AD the end-effector using both MCAs based on MPC WTR and WOTR: (a) *x*-axis; (b) *y*-axis; (c) *z*-axis; (d) *Roll*-angle; (e) *Pitch*-angle; (f) *Yaw*-angle.

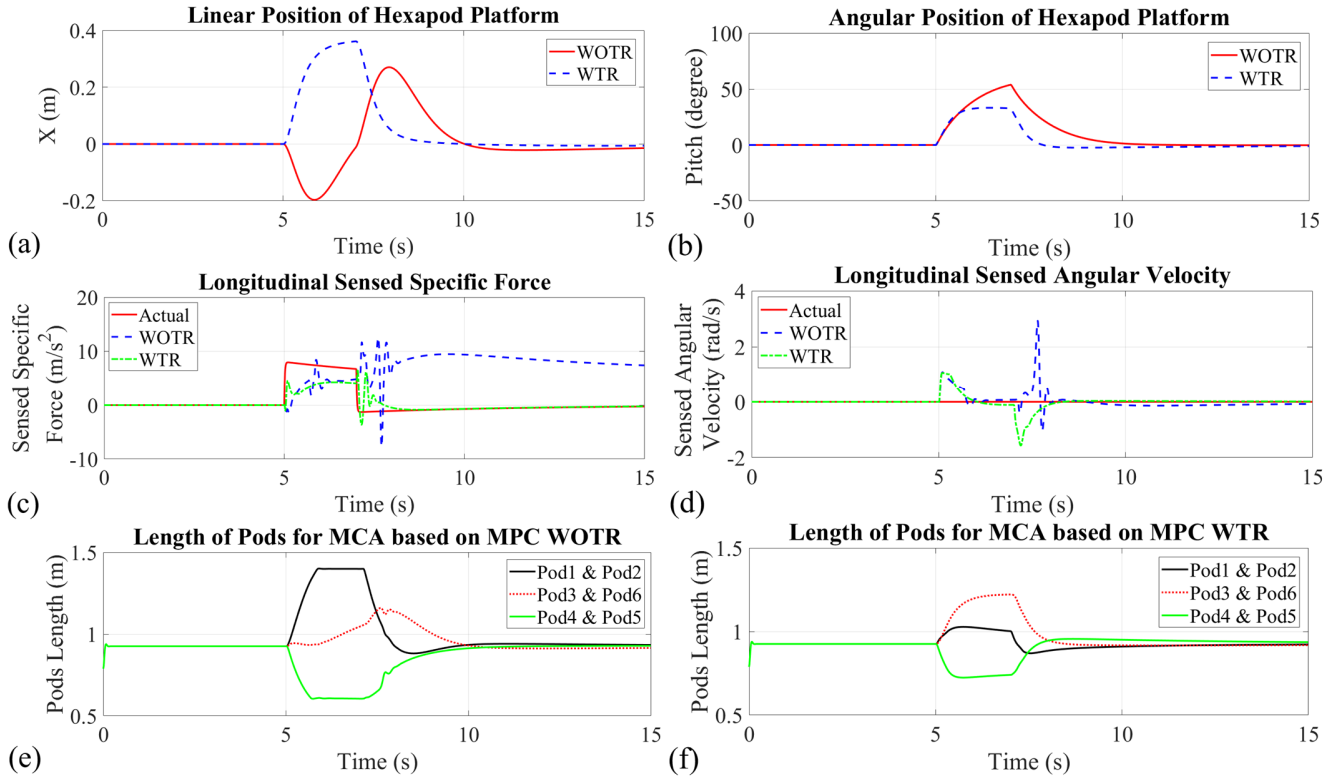


Fig. 6. The stability of the MCAs based on MPC WTR and WOTR: (a) LD along *x*-axis; (b) AD along *pitch*-angle; (c) SSF along *x*-axis; (d) SAV along *pitch*-angle; (e) Pods' length of MCA based on MPC WOTR; (f) Pods' length of MCA based on MPC WTR.

motion feeling while respecting the workspace boundaries compared to the existing MCA based on MPC. This method is appropriate for the urban motion scenario when there are many stops and starts moving involved (accelerations and deaccelerations) such as driving in traffic.

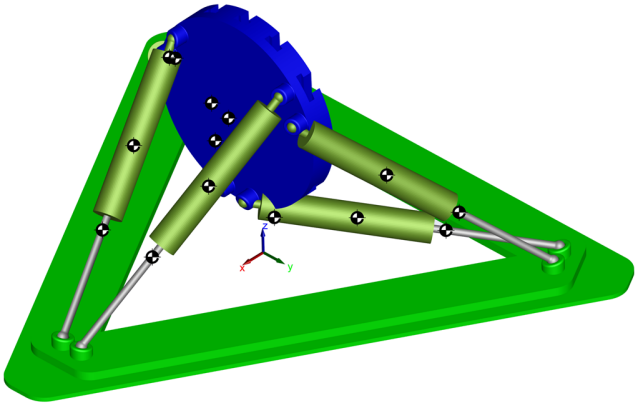


Fig. 7. The final configuration of the Hexapod SBMP using MCA based on MPC WOTR.

V. Conclusion

The MCA based on MPC WTR is proposed in this study to regenerate the motion signal in urban area where there are sudden decelerations/accelerations (stop and start vehicle movements). The MCA based on MPC WOTR is recently used to regenerate the motion feeling for the driver of the SBMP, but these MCAs are not suitable for urban motion scenario. The motion fluctuation and exceeding the joints' limitations using the MCA based on MPC WOTR (weighting parameters and states) are the main problems of the current models. The absence of the terminal states causes the movement of the end-effector towards infinity when there is a big motion signal including decelerations/accelerations in heavy-traffic situations. Considering the terminal states guarantees the returning of the end-effector to the neutral position at the end of the prediction horizon. Also, the weighting parameters of the MCA based on MPC WOTR should be chosen conservatively to keep the end-effector inside the workspace area which can cause inefficient workspace movement and motion feeling error for the driver of the SBMP. The consideration of the terminal conditions enhances the ability of the model to return to the neutral positions at the end of the prediction horizon, and the definition of the terminal weighting parameters eliminates the necessity of the conservative weight tuning to keep the end-effector and joints within their limitations. The newly designed MCA based on MPC WTR is capable of using the most parts of the workspace area while respecting the workspace boundaries of the SBMP as the end-effector can return to the neutral position at the end of the prediction horizon and be ready for the next movement. At last, the stability of the model is studied using the terminal conditions (weighting parameters and states). The results show the effectiveness of the proposed method in terms of respecting the limitations of the SBMP as well as regenerating the more accurate motion signals.

References

[1] L. Nehaoua, H. Mohellebi, A. Amouri, H. Arioui, S. Espié, and A. Kheddar, "Design and control of a small-clearance driving simulator," *IEEE Transactions on Vehicular Technology,* vol. 57, no. 2, pp. 736-746, 2008.

[2] H. Asadi, S. Mohamed, C. P. Lim, and S. Nahavandi, "Robust optimal motion cueing algorithm based on the linear quadratic regulator method and a genetic algorithm," *IEEE Transactions on Systems, Man, and Cybernetics: Systems,* vol. 47, no. 2, pp. 238-254, 2016.

[3] M. R. C. Qazani *et al.*, "Kinematic analysis and workspace determination of hexarot-a novel 6-DOF parallel manipulator with a rotation-symmetric arm system," *Robotica,* vol. 33, no. 8, pp. 1686-1703, 2015.

[4] C.-Y. Tsai, C.-C. Wong, C.-J. Yu, C.-C. Liu, and T.-Y. Liu, "A hybrid switched reactive-based visual servo control of 5-DOF robot manipulators for pick-and-place tasks," *IEEE Systems Journal,* vol. 9, no. 1, pp. 119-130, 2014.

[5] M. R. C. Qazani, S. Pedrammehr, H. Abdi, and S. Nahavandi, "Performance Evaluation and Calibration of Gantry-Tau Parallel Mechanism," *Iranian Journal of Science and Technology, Transactions of Mechanical Engineering,* pp. 1-15, 2019.

[6] J.-P. Merlet, *Parallel robots*. Springer Science & Business Media, 2006.

[7] S. Pedrammehr, M. R. C. Qazani, H. Asadi, and S. Nahavandi, "Kinematic manipulability analysis of hexarot simulators," in *The 20th IEEE International Conference on Industrial Technology, IEEE-ICIT 2019*, 2019, pp. 13-15.

[8] B. Conrad and S. F. Schmidt, "A study of techniques for calculating motion drive signals for flight simulators," 1971.

[9] S. Casas, I. Coma, C. Portalés, and M. Fernández, "Towards a simulation-based tuning of motion cueing algorithms," *Simulation Modelling Practice and Theory,* vol. 67, pp. 137-154, 2016.

[10] A. Mohammadi, H. Asadi, S. Mohamed, K. Nelson, and S. Nahavandi, "OpenGA, a C++ genetic algorithm library," in *2017 IEEE International Conference on Systems, Man, and Cybernetics (SMC)*, 2017, pp. 2051-2056: IEEE.

[11] H. Asadi *et al.*, "A Particle Swarm Optimization-based washout filter for improving simulator motion fidelity," in *2016 IEEE International Conference on Systems, Man, and Cybernetics (SMC)*, 2016, pp. 001963-001968: IEEE.

[12] R. V. Parrish, J. E. Dieudonne, and D. J. Martin Jr, "Coordinated adaptive washout for motion simulators," *Journal of aircraft,* vol. 12, no. 1, pp. 44-50, 1975.

[13] H. R. Baghaee, M. Mirsalim, and G. B. Gharehpetian, "Performance improvement of multi-DER microgrid for small-and large-signal disturbances and nonlinear loads: Novel complementary control loop and fuzzy controller in a hierarchical droop-based control scheme," *IEEE Systems Journal,* vol. 12, no. 1, pp. 444-451, 2016.

[14] S. Muyeen and A. Al-Durra, "Modeling and control strategies of fuzzy logic controlled inverter system for grid interconnected variable speed wind generator," *IEEE systems journal,* vol. 7, no. 4, pp. 817-824, 2013.

[15] L. A. Zadeh, "Fuzzy logic," *Computer,* vol. 21, no. 4, pp. 83-93, 1988.

[16] H. Asadi, C. P. Lim, S. Mohamed, D. Nahavandi, and S. Nahavandi, "Increasing Motion Fidelity in Driving Simulators Using a Fuzzy-Based Washout Filter," *IEEE Transactions on Intelligent Vehicles,* vol. 4, no. 2, pp. 298-308, 2019.

[17] H. Asadi, S. Mohamed, and S. Nahavandi, "Incorporating human perception with the motion washout filter using fuzzy logic control," *IEEE/ASME Transactions on Mechatronics,* vol. 20, no. 6, pp. 3276-3284, 2015.

[18] T.-S. Hwang, S.-K. Yeh, J.-R. Lin, and W.-P. Su, "Adaptive motion washout filter design by using self-tuning fuzzy control," in *2009 IEEE/ASME International Conference on Advanced Intelligent Mechatronics*, 2009, pp. 811-815: IEEE.

[19] W. R. Sturgeon, "Controllers for aircraft motion simulators," *Journal of Guidance and Control,* vol. 4, no. 2, pp. 184-191, 1981.

[20] L. Reid and M. Nahon, "Flight simulation motion-base drive algorithms: part 1. developing and testing equations," University of Toronto1985.

[21] H. Asadi, S. Mohamed, D. Rahim Zadeh, and S. Nahavandi, "Optimisation of nonlinear motion cueing algorithm based on genetic algorithm," *Vehicle System Dynamics,* vol. 53, no. 4, pp. 526-545, 2015.

[22] H. Asadi, S. Mohamed, K. Nelson, S. Nahavandi, and M. Oladazimi, "An optimal washout filter based on genetic algorithm compensators for improving simulator driver perception," in *DSC 2015: Proceedings of the Driving Simulation Conference &*

Exhibition, 2015, pp. 1-10: Max Planck Institute for the Advancement of Science.
[23] M. Dagdelen, G. Reymond, A. Kemeny, M. Bordier, and N. Maïzi, "Model-based predictive motion cueing strategy for vehicle driving simulators," *Control Engineering Practice,* vol. 17, no. 9, pp. 995-1003, 2009.
[24] Z. Fang and A. Kemeny, "Explicit MPC motion cueing algorithm for real-time driving simulator," in *Proceedings of The 7th International Power Electronics and Motion Control Conference*, 2012, vol. 2, pp. 874-878: IEEE.
[25] D. Krupchanka, M. Katliar, D. Krupchanka, M. Katliar, D. Krupchanka, and M. Katliar, "Comparison between filter-and optimization-based motion cueing algorithms for driving simulation," *Transportation Research,* vol. 28, no. Part F, p. 746, 2018.
[26] A. Mohammadi, H. Asadi, S. Mohamed, K. Nelson, and S. Nahavandi, "Optimizing model predictive control horizons using genetic algorithm for motion cueing algorithm," *Expert Systems with Applications,* vol. 92, pp. 73-81, 2018.
[27] C. Rengifo, J.-R. Chardonnet, D. Paillot, H. Mohellebi, and A. Kemeny, "Solving the Constrained Problem in Model Predictive Control based Motion Cueing Algorithm with a Neural Network Approach," 2018.
[28] M. R. C. Qazani, H. Asadi, and S. Nahavandi, "A Decoupled Linear Model Predictive Control-based Motion Cueing Algorithm for Simulation-based Motion Platform with Limitted Workspace."
[29] M. R. C. Qazani, H. Asadi, and S. Nahavandi, "A New Gantry-Tau-Based Mechanism Using Spherical Wrist and Model Predictive Control-Based Motion Cueing Algorithm," *Robotica,* pp. 1-22, 2019.
[30] M. R. C. Qazani, H. Asadi, and S. Nahavandi, "High-Fidelity Hexarot Simulation-Based Motion Platform Using Fuzzy Incremental Controller and Model Predictive Control-Based Motion Cueing Algorithm," *IEEE Systems Journal,* 2019.
[31] M. R. C. Qazani, H. Asadi, S. Khoo, and S. Nahavandi, "A Linear Time-Varying Model Predictive Control-Based Motion Cueing Algorithm for Hexapod Simulation-Based Motion Platform," *IEEE Transactions on Systems, Man, and Cybernetic: Systems,* 2019.
[32] M. R. C. Qazani, H. Asadi, and S. Nahavandi, "A Model Predictive Control-Based Motion Cueing Algorithm with Consideration of Joints' limitations for Hexapod Motion Platform," in *2019 IEEE International Conference on Systems, Man and Cybernetics (SMC)*, 2019, pp. 708-713: IEEE.
[33] M. R. C. Qazani, S. Pedrammehr, and M. J. Nategh, "An investigation on the motion error of machine tools' hexapod table," *International Journal of Precision Engineering and Manufacturing,* vol. 19, no. 4, pp. 463-471, 2018.
[34] W. Kwon and A. Pearson, "A modified quadratic cost problem and feedback stabilization of a linear system," *IEEE Transactions on Automatic Control,* vol. 22, no. 5, pp. 838-842, 1977.
[35] W. Kwon and A. Pearson, "On feedback stabilization of time-varying discrete linear systems," *IEEE Transactions on Automatic Control,* vol. 23, no. 3, pp. 479-481, 1978.
[36] B. Kouvaritakis and M. Cannon, "Model predictive control," *Switzerland: Springer International Publishing,* 2016.
[37] W. H. Kwon, A. Bruckstein, and T. Kailath, "Stabilizing state-feedback design via the moving horizon method," *International Journal of Control,* vol. 37, no. 3, pp. 631-643, 1983.
[38] W. H. Kwon and D. G. Byun, "Receding horizon tracking control as a predictive control and its stability properties," *International Journal of Control,* vol. 50, no. 5, pp. 1807-1824, 1989.
[39] H. Asadi, S. Mohamed, C. P. Lim, and S. Nahavandi, "A review on otolith models in human perception," *Behavioural brain research,* vol. 309, pp. 67-76, 2016.
[40] H. Asadi, S. Mohamed, C. P. Lim, S. Nahavandi, and E. Nalivaiko, "Semicircular canal modeling in human perception," *Reviews in the Neurosciences,* vol. 28, no. 5, pp. 537-549, 2017.
[41] J. A. Houck, R. J. Telban, and F. M. Cardullo, "Motion cueing algorithm development: Human-centered linear and nonlinear approaches," 2005.
[42] L. Magni and R. Scattolini, "Stabilizing decentralized model predictive control of nonlinear systems," *Automatica,* vol. 42, no. 7, pp. 1231-1236, 2006.
[43] C. Schmid and L. T. Biegler, "Quadratic programming methods for reduced hessian SQP," *Computers & chemical engineering,* vol. 18, no. 9, pp. 817-832, 1994.
[44] S. Pedrammehr, M. R. C. Qazani, H. Asadi, and S. Nahavandi, "Control system development of a hexarotbased high-G centrifugal simulator," in *The 20th IEEE International Conference on Industrial Technology IEEE-ICIT 2019*, 2019.
[45] H. Asadi, C. P. Lim, A. Mohammadi, S. Mohamed, S. Nahavandi, and L. Shanmugam, "A genetic algorithm–based nonlinear scaling method for optimal motion cueing algorithm in driving simulator," *Proceedings of the Institution of Mechanical Engineers, Part I: Journal of Systems and Control Engineering,* vol. 232, no. 8, pp. 1025-1038, 2018.
[46] H. Asadi *et al.*, "A Model Predictive Control-based Motion Cueing Algorithm using an optimized Nonlinear Scaling for Driving Simulators," in *2019 IEEE International Conference on Systems, Man and Cybernetics (SMC)*, 2019, pp. 1245-1250: IEEE.
[47] M. Katliar, F. M. Drop, H. Teufell, M. Diehl, and H. H. Bülthoff, "Real-Time Nonlinear Model Predictive Control of a Motion Simulator Based on a 8-DOF Serial Robot," in *2018 European Control Conference (ECC)*, 2018, pp. 1529-1535: IEEE.



Mohammad Reza Chalak Qazani received the Bachelor of Engineering in manufacturing and production from University of Tabriz, Tabriz, Iran in 2010 and the master's degree in robotic and mechanical engineering from the Tarbiat Modares University, Tehran, Iran, in 2013.

He is currently a Ph.D. student in the Institute for Intelligent Systems Research and Innovation (IISRI), Deakin University model predictive control, motion cueing algorithm and soft computing controllers.



Houshyar Asadi received the Bachelor of Engineering degree (First Class Hons.) in electrical-control systems in 2008, and Master degree in Industrial Electronic and Control Engineering from University of Malaya in 2012. He received the Ph.D. degree in human perception-based washout filtering using Artificial intelligence (AI) from the Institute for Intelligent Systems Research and Innovation (IISRI), Deakin University, Australia, in 2015.

He is currently a Senior Research Fellow of Control and Motion Analysis with the IISRI, Deakin University. His current research interests include computational intelligence, motion-based simulator technologies, motion cueing algorithms, robotics, control, and human factors in virtual environments.



Saeid Nahavandi received a Ph.D. from Durham University, U.K. in 1991. He is an Alfred Deakin Professor, Pro Vice-Chancellor, Chair of Engineering, and the Founding Director of the Institute for Intelligent Systems Research and Innovation at Deakin University. His research interests include modeling of complex systems, robotics and haptics. He has published over 900 scientific papers in various international journals and conferences.

Professor Nahavandi is Editor-In-Chief: IEEE SMC Magazine, the Senior Associate Editor: IEEE Systems Journal, Associate Editor of IEEE Transactions on Systems, Man and Cybernetics: Systems, and IEEE Press Editorial Board member. Professor Nahavandi is a Fellow of IEEE (FIEEE), Engineers Australia (FIEAust), the Institution of Engineering and Technology (FIET). Saeid is a Fellow of the Australian Academy of Technology and Engineering (ATSE).